

MOTION-R1: ENHANCING MOTION GENERATION WITH DECOMPOSED CHAIN-OF-THOUGHT AND RL BINDING

Runqi Ouyang^{1,2,3*} Haoyun Li^{1,2,3*} Zhenyuan Zhang^{4,5*} Xiaofeng Wang⁴
Zeyu Zhang⁴ Zheng Zhu^{4†} Guan Huang⁴ Sirui Han⁵ Xingang Wang^{1,3‡}

¹Institute of Automation, Chinese Academy of Sciences

²School of Artificial Intelligence, University of Chinese Academy of Sciences

³Luoyang Institute for Robot and Intelligent Equipment

⁴GigaAI ⁵Hong Kong University of Science and Technology

ABSTRACT

Text-to-Motion generation has become a fundamental task in human-machine interaction, enabling the synthesis of realistic human motions from natural language descriptions. Although recent advances in large language models and reinforcement learning have contributed to high-quality motion generation, two major challenges remain. Existing approaches often fail to capture the temporal and causal complexities inherent in natural language, leading to oversimplified or incoherent motions. Additionally, RL-based methods are frequently overly complex, hindering their scalability and adaptability across various motion generation tasks. To address these challenges, we propose **Motion-R1**, a novel framework that combines decomposed Chain-of-Thought reasoning with reinforcement learning to enhance both the quality and interpretability of generated motions. Specifically, we introduce the **Decomposed CoT Data Engine**, which leverages an automated pipeline to synthesize high-quality reasoning data, allowing the model to better capture the temporal dependencies and causal relationships of human motion. We also propose **RL Binding**, a reinforcement learning strategy that incorporates multi-modal text-motion alignment into the RL reward function, guiding the model to produce motions that are both semantically accurate and motionally realistic. Extensive experiments across benchmark datasets demonstrate that Motion-R1 achieves state-of-the-art performance, with a 3.5% improvement in MM-Dist on HumanML3D and improvements in R-Precision and FID on KIT-ML and BABEL, surpassing existing methods across key metrics and highlighting its superior capability in handling complex motion generation tasks.

1 INTRODUCTION

Text-to-Motion (T2M) generation Guo et al. (2022c); Tevet et al. (2023); Guo et al. (2022a) has emerged as a fundamental task in human-machine interaction, enabling the synthesis of realistic human motions from natural language descriptions. Driven by rapid advancements in large language models (LLMs) Achiam et al. (2023); Li et al. (2023), recent T2M approaches Jiang et al. (2023); Wang et al. (2024); Wu et al. (2024) have made significant strides in generating high-fidelity motions that align with complex textual instructions. Reinforcement learning (RL) Kaelbling et al. (1996) provides a promising approach to enhance motion generation by optimizing it for motion quality. Recent works Liu et al. (2024); Haoru Wang et al. (2025) have successfully integrated RL into motion generation, improving both text adherence and motion quality by aligning with human perceptual preferences. However, despite significant advancements in motion generation, current methods still face two major challenges.

*Equal contribution.

†Corresponding authors: zhengzhu@ieee.org, xingang.wang@ia.ac.cn.

‡Project page: <https://motion-r1.github.io/>

(1) Existing approaches predominantly rely on end-to-end supervised learning Ahn et al. (2017); Hong et al. (2022); Ahuja & Morency (2019), directly mapping textual inputs to motion sequences. While this approach is simple, it fails to capture the deeper temporal and causal relationships inherent in natural language. For instance, a high-level task like "making a cup of coffee" involves a series of connected sub-actions (e.g., reaching, grasping, pouring, stirring, placing), which require careful temporal ordering and causal reasoning. However, these methods often struggle to effectively decompose such tasks, resulting in oversimplified or incoherent motion generation.

(2) RL-based methods, such as MotionRL Liu et al. (2024) and MotionCritic Haoru Wang et al. (2025), demonstrate improvements in motion quality but are often overly complex and over-engineered. These designs, though effective, limit their adaptability to real-world applications. The intricate nature of these RL models makes them difficult to scale and deploy across a wide range of motion generation tasks, especially when simplicity and efficiency are needed.

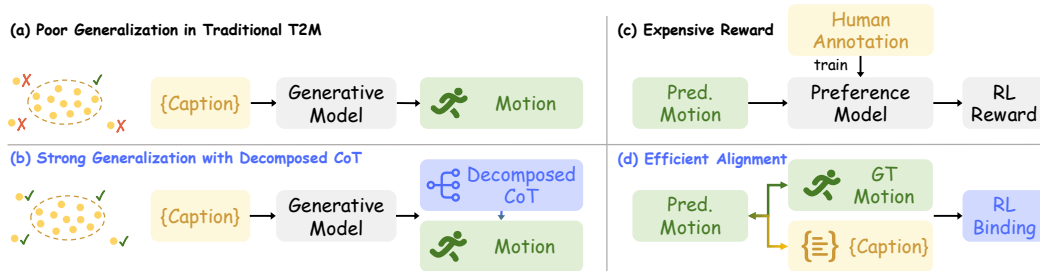


Figure 1: **Comparison of traditional approaches and our Motion-R1 framework.** (a) Traditional end-to-end models exhibit poor generalization on out-of-distribution motions. (b) Our Decomposed CoT Data Engine enables strong generalization by structuring high-level instructions into intermediate reasoning steps. (c) Existing RL-based methods rely on expensive human annotations to train preference models for reward signals. (d) Our RL Binding mechanism achieves efficient multi-modal alignment without additional annotation cost.

Our motivation is to advance motion generation by introducing a novel framework, **Motion-R1** that effectively addresses the key challenges in the field, as shown in Figure 1.

To tackle the first challenge, we propose a **Decomposed CoT Data Engine** which synthesizes high-quality, step-by-step reasoning data. Inspired by the recent success of Chain-of-Thought (CoT) Wei et al. (2022) prompting in enhancing reasoning capabilities of LLMs, we hypothesize that explicitly modeling intermediate reasoning steps can similarly benefit motion generation tasks. By decomposing high-level instructions into structured action plans, our engine leverages an automated CoT annotation pipeline that employs LLMs to generate structured motion planning paths, enabling models to better capture temporal dependencies, causal relationships, and fine-grained semantic nuances embedded in language. This approach not only enhances the realism and coherence of the generated motions but also reduces reliance on expensive manual annotation, making the process more efficient and scalable.

To address the second challenge, we introduce **RL Binding**, a novel reinforcement learning strategy that enhances motion generation by incorporating a multi-modal alignment mechanism within the RL framework. RL Binding simultaneously aligns the generated motion sequences with both the ground-truth motions and the corresponding textual descriptions. This dual alignment process ensures that the generated motions not only stay temporally consistent with real-world actions but also faithfully capture the semantic meaning conveyed in the textual instructions. By embedding these alignments directly into the RL reward function (specifically, the *motion similarity reward*, the *semantic similarity reward*, and the *format reward*), RL Binding guides the model to produce motions that are both semantically accurate and motionally realistic. This streamlined design simplifies the optimization process, improving both the quality and interpretability of the generated motions, while offering a highly adaptable and efficient solution for real-world applications.

Moreover, to demonstrate the effectiveness of our approach, we conduct extensive experiments on multiple benchmark datasets. Our method achieves a 3.5% improvement in MM-Dist on HumanML3D Guo et al. (2022a), while also setting new state-of-the-art records in R-Precision and FID on both KIT-ML Plappert et al. (2016) and BABEL Punnakkal et al. (2021). These results

highlight the superiority of our method in both motion quality and task performance, showcasing its strong potential for real-world applications.

In general, our work’s contributions can be summarized in the following three folds:

- **Decomposed CoT Data Engine:** We introduce a novel framework for synthesizing high-quality, step-by-step reasoning data. By leveraging an automated CoT annotation pipeline powered by LLMs, our approach effectively captures the temporal dependencies and causal relationships inherent in motion generation. This method significantly improves the quality of generated motions while reducing the reliance on costly manual annotation, making the process more efficient and scalable.
- **RL Binding Strategy:** We propose RL Binding, a novel reinforcement learning strategy that integrates multi-modal text-motion alignment into the reward function via the *motion similarity reward*, the *semantic similarity reward*, and the *format reward*, effectively guiding the model to generate motions that better adhere to textual instructions while maintaining high motion quality. The simplicity and effectiveness of RL Binding enhance the model’s ability to optimize across both modalities, resulting in improved precision and interpretability in motion generation.
- **Comprehensive Experimental Validation:** We conduct extensive experiments across multiple benchmark datasets, demonstrating the effectiveness of Motion-R1. On HumanML3D, it achieves a **3.5% improvement in MM-Dist**, with Diversity and R-Precision metrics reaching state-of-the-art or on-par performance. On KIT-ML, Motion-R1 sets **new records in R-Precision and FID**, outperforming existing methods. On BABEL, it achieves **state-of-the-art performance across all key metrics**, including R-Precision, FID, MM-Dist, and Diversity. These results highlight the model’s superior ability to generate diverse, high-fidelity, and semantically aligned motions.

2 RELATED WORK

Multimodal Large Language Models Recently, multimodal large language models (MLLMs) Wu et al. (2023); Koh et al. (2023); Tang et al. (2025) have shown impressive performance in various tasks, including text generation, reasoning, and even multimodal tasks. For example, models like GPT-4 Achiam et al. (2023) and BLIP-2 Li et al. (2023) have demonstrated the ability to understand and generate text and images. While recent MLLMs have significantly improved their perception and generation capabilities across diverse modalities, many complex real-world tasks demand not only understanding but also reasoning Banerjee et al. (2021); Xiong et al. (2024). Consequently, enhancing the reasoning abilities of MLLMs has become an important research direction.

Building on the success of CoT Wei et al. (2022) prompting in NLP, researchers have explored extending CoT-style reasoning to multimodal settings. For instance, models like LLaVA-CoT Xu et al. (2025) introduce a novel vision-language model capable of performing autonomous, structured, and multistage reasoning by decomposing complex questions into four stages: summary, caption, reasoning, and conclusion.

While structured reasoning enhances interpretability and controllability, recent studies Tan et al. (2025); Pan et al. (2025); Liu et al. (2025) show that it can be further optimized through reinforcement learning. Building on GRPO Guo et al. (2025), we introduce a decomposed CoT paradigm for structured motion reasoning and an RL Binding mechanism, together enabling interpretable and semantically aligned motion synthesis.

Text-guided 3D Human Motion Generation Text-guided 3D human motion generation has become a key research focus in recent years. Early methods Ahn et al. (2017); Ghosh et al. (2023) primarily relied on generative adversarial networks Goodfellow et al. (2014) to synthesize human motion from text descriptions. These methods often struggled with issues such as limited diversity.

To address these challenges, diffusion models Ho et al. (2020) have gained popularity in this field. Notable works Zhou & Wang (2022); Kim et al. (2023); Dabral et al. (2023) include MDM Tevet et al. (2023), which first applies diffusion modeling to motion synthesis; MotionDiffuse Zhang et al. (2022a) improves temporal consistency; MotionChain Jiang et al. (2024) explores fine-grained structure and staged modeling; and MoMask Guo et al. (2024) employs masking strategies for improved

training efficiency. However, these methods often rely on complex architectures and extensive training data and are limited by their motion initialization.

In parallel, VQ-VAE-based methods Guo et al. (2022a); Hong et al. (2022); Petrovich et al. (2022); Guo et al. (2022b); Athanasiou et al. (2022); Zhang et al. (2024b; 2025b); Li et al. (2025); Zhang et al. (2024d;a) discretize motion representations to facilitate efficient sequence modeling and better alignment with language, providing a more interpretable latent space. Building on this, LLMs have been integrated into the generation process to enhance the quality and control of generated motions. For instance, T2M-GPT Zhang et al. (2023a) combines VQ-VAE with GPT in a two-stage framework for high-quality generation. Subsequent works such as MotionDiffuse Zhang et al. (2022b), MotionCLIP Tevet et al. (2022), and MotionGPT Jiang et al. (2023) integrate diffusion modeling, contrastive learning, and Transformer architectures to enhance fidelity and semantic consistency further. MotionAgent Wu et al. (2024) further incorporates semantic planning for robust generalization in complex task scenarios.

As the development of reinforcement learning, several approaches have emerged to enhance text-to-motion generation. InstructMotion Mao et al. (2024) uses trial-and-error in reinforcement learning for generalizable motion generation. AToM Han et al. (2024b) enhances the alignment between generated motion and text prompts using rewards from vision-language models. ReinDiffuse Han et al. (2024a) applies reinforcement learning to guide diffusion for motion synthesis. RLPF Yue et al. (2025) utilizes physical feedback from simulation environments to align motion models with humanoid policies. MotionRL Liu et al. (2024) leverages PPO Schulman et al. (2017) to improve generation based on human preferences and prior knowledge. MotionCritic Haoru Wang et al. (2025) introduces a critic model to align motions with textual semantics via preference optimization.

Despite recent advances, T2M methods largely rely on end-to-end mapping and lack explicit reasoning over complex instructions Zhang et al. (2024c; 2025a). Our approach addresses this by combining a decomposed CoT mechanism for interpretable motion reasoning with an RL Binding strategy for efficient multimodal alignment, enabling coherent and semantically grounded motion generation without costly annotations.

3 METHOD

3.1 MOTION-R1 FRAMEWORK

Motion-R1 comprises two core components: a pre-trained motion tokenizer and an LLM equipped with action-oriented reasoning capabilities. The motion tokenizer discretizes continuous motion sequences into motion tokens and reconstructs them back into smooth, coherent trajectories. Meanwhile, the LLM is designed to perform structured reasoning over natural language instructions, enabling it to decompose complex action descriptions into finer-grained and logically ordered sub-actions, a process we term decomposed CoT reasoning. Based on this structured interpretation, the model generates high-quality motion token sequences that faithfully reflect the intended behavior.

As shown in Figure 2, our framework consists of two training stages. we employ the **Decomposed CoT Data Engine**, a novel automated pipeline for synthesizing high-quality, step-by-step reasoning data, which enables cold-start supervised tuning of the LLM to produce reasoning-augmented outputs in the `<think>`, `<output>`, and `<Motion>` format. By distilling the reasoning capabilities of LLMs into structured motion planning paths, this stage provides interpretable supervision and reduces reliance on costly manual annotation, enabling efficient and scalable pretraining of LLMs.

In the second stage, we refine the LLM via reinforcement learning using our proposed **RL Binding** strategy. Building on the GRPO Shao et al. (2024) framework, RL Binding streamlines optimization by embedding multi-modal alignment directly into the reward function, jointly evaluating embedded motion similarity with ground-truth trajectories and semantic consistency with textual descriptions. Unlike prior RL-based methods that rely on costly human annotations for preference models, RL Binding efficiently guides the model to generate motions that are both semantically faithful and motionally coherent. This design maintains simplicity and adaptability while enhancing precision, interpretability, and overall motion quality.

By combining the Decomposed CoT Data Engine and RL Binding, Motion-R1 effectively captures temporal and causal structure while ensuring semantic fidelity and motion realism, providing a uni-

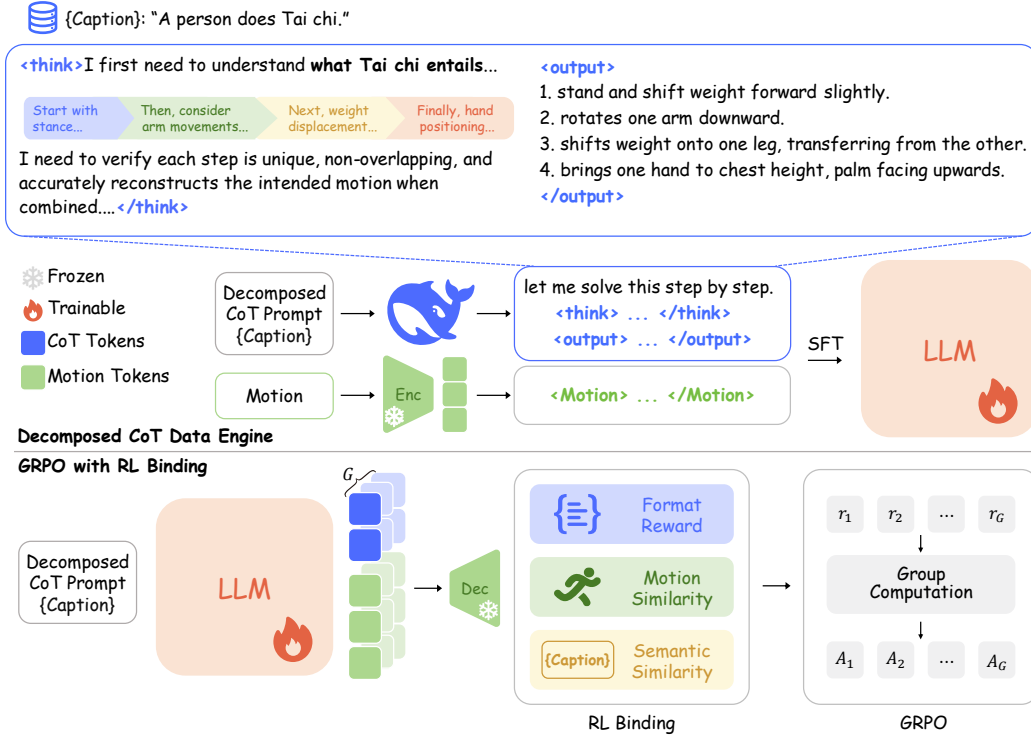


Figure 2: **Overview of the Motion-RI framework.** Our method introduces two key innovations: (1) a Decomposed CoT Data Engine that generates structured motion planning traces (including <think>, <output>, and <Motion> tokens) via LLM reasoning, enabling fine-grained temporal and causal decomposition; (2) an RL Binding mechanism with GRPO-based training that streamlines optimization via embedded multi-modal alignment, ensuring semantic accuracy and motion realism without human annotations.

fied framework for coherent, interpretable, and high-quality motion generation without the need for costly human annotations.

3.2 MOTION TOKENIZER

To integrate motion data, which differs significantly from natural language in structure and modality, into the LLM framework, we adopt a VQ-VAE architecture as our motion tokenizer. This approach has been widely adopted in Zhang et al. (2023a); Jiang et al. (2023); Guo et al. (2024); Wu et al. (2024) and proven effective for 3D human motion data modeling.

The motion tokenizer comprises an encoder E and a decoder D . Given an input motion sequence $\mathbf{m}_{1:T} \in \mathbb{R}^{T \times D}$, with T frames of D dimensions each, the encoder E maps the sequence to a latent representation $\mathbf{z}_{1:(T/l)} \in \mathbb{R}^{(T/l) \times d}$, where l is the temporal downsampling rate and d is the number of latent dimensions. Each latent vector \mathbf{z}_i is then quantized using a learnable codebook $\mathbf{C} = \{\mathbf{c}_n\}_{n=1}^N$, where N is the codebook size and $\mathbf{c}_n \in \mathbb{R}^d$ represents a discrete motion token. The quantization selects the nearest code vector to each embedding:

$$\hat{\mathbf{z}}_i = \arg \min_{\mathbf{c}_n \in \mathbf{C}} \|\mathbf{z}_i - \mathbf{c}_n\|_2 \quad (1)$$

The original motion sequence is reconstructed as $\hat{\mathbf{m}}_{1:T} = D(\hat{\mathbf{z}}_{1:(T/l)})$. Following Zhang et al. (2023a), we train the VQ-VAE model using a composite objective that includes a reconstruction loss $L_{\text{reconstruct}}$, a codebook commitment loss L_{commit} , and an embedding loss L_{embed} :

$$L_{\text{vq}} = L_{\text{reconstruct}} + L_{\text{commit}} + L_{\text{embed}} \quad (2)$$

Here, $L_{\text{reconstruct}}$ includes a smoothed L1 loss with velocity regularization to improve generation quality. To ensure stable and efficient training, we follow Zhang et al. (2023a) to incorporate exponential moving average (EMA) updates for the codebook along with codebook reset strategies.

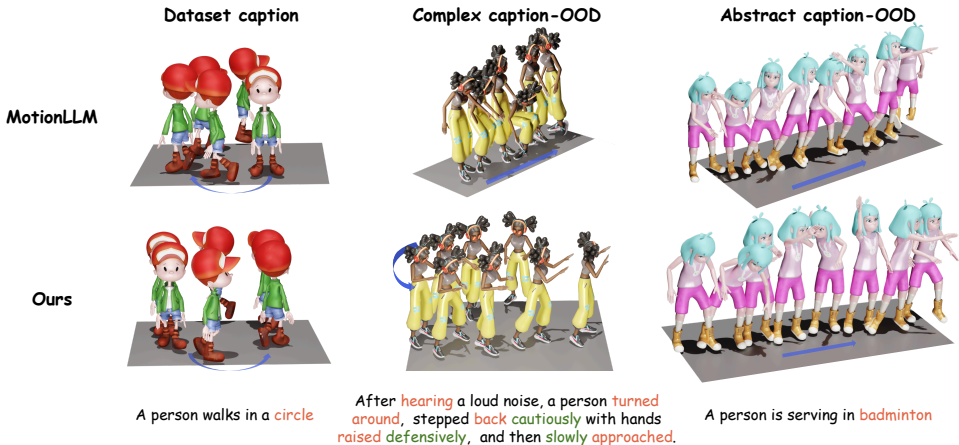


Figure 3: **Visualization comparisons** with MotionLLM Wu et al. (2024) on in-distribution and out-of-distribution prompts.

3.3 DECOMPOSED CoT DATA ENGINE

We introduce the **Decomposed CoT Data Engine**, an automated module for generating structured reasoning traces to guide text-to-motion generation. This engine leverages the reasoning and semantic planning capabilities of LLMs to transform free-form motion descriptions into high-quality, step-by-step CoT action plans, providing intermediate supervision that bridges language and motion.

The engine starts by augmenting existing motion-language datasets using prompt-based LLM queries. We design comprehensive prompts that instruct the LLM to decompose tasks into logically ordered sub-actions while respecting temporal dependencies and action semantics. These prompts include clear instructions, output format constraints, and in-context examples to ensure structured reasoning outputs. The complete details of the prompt are provided in the Appendix A.2 material.

Generated CoT traces are then evaluated through an automated quality control pipeline. We employ DeepSeek-R1 Guo et al. (2025) to assess each trace for relevance, logical consistency, and conciseness. Traces that exhibit redundancy, overthinking, or verbosity are filtered and regenerated until they meet quality standards. This iterative filtering and regeneration process serves as our self-verification mechanism, ensuring high-quality training data. Figure 2 illustrates the full Motion-R1 pipeline, with the Decomposed CoT Data Engine highlighted to show the structured reasoning trace generation process. For the task “A person does Tai chi”, the engine identifies the main action, decomposes it into sub-actions such as “stand up”, “arm movements”, “weight displacement”, and “hand positioning”, and further elaborates each sub-action with motion-relevant details like movement direction and involved body parts.

Each validated CoT trace is paired with its original textual description and corresponding motion sequence, forming triplets of the form (description, decomposed CoT, motion). By distilling structured action plans, the Decomposed CoT Data Engine enables the model to capture fine-grained temporal and causal dependencies directly from language, significantly improving controllability, interpretability, and generalization in complex motion generation, while drastically reducing reliance on costly manual annotation.

3.4 TRAINING STRATEGY

3.4.1 COLD-START TRAINING WITH DECOMPOSED CoT

Inspired by DeepSeek-R1-Zero Guo et al. (2025), we first attempt end-to-end RL training to induce decomposed CoT reasoning and motion generation purely from reward signals. Yet this setting proves unstable, as the model often fails to produce coherent reasoning or valid motion tokens. This instability stems from two factors: motion generation requires long, structured sequences rather than short symbolic outputs, and motion tokens are newly introduced symbols with insufficiently trained embeddings to bridge the modality gap.

To mitigate these issues, we adopt a cold-start strategy based on supervised fine-tuning. Leveraging curated triplets of captions, decomposed CoT traces, and motions, we bootstrap the model’s

capacity to produce structured reasoning and valid motion outputs, providing a stable foundation for subsequent RL optimization.

3.4.2 GRPO-BASED TRAINING WITH RL BINDING

To enhance alignment between textual instructions and generated motions without incurring costly human annotations, RL Binding formulates text-to-motion generation as a reinforcement learning problem, employing GRPO Shao et al. (2024) to optimize the generation policy efficiently.

For each text prompt q , a group of G outputs $\{o_1, o_2, \dots, o_G\}$ are sampled from the old policy model π_{old} . Each output is assigned a scalar reward, yielding a reward vector $\mathbf{r} = \{r_1, r_2, \dots, r_G\}$, computed by task-specific reward functions that evaluate the quality of each output. GRPO then updates the policy model by maximizing the following clipped objective:

$$\mathcal{J}_{\text{GRPO}}(\theta) = \mathbb{E}_{\mathbf{c}} \left[\frac{1}{G} \sum_{i=1}^G \min \left(\frac{\pi_{\theta}(o_i|q)}{\pi_{\text{old}}(o_i|q)} \hat{A}_i, \text{clip} \left(\frac{\pi_{\theta}(o_i|q)}{\pi_{\text{old}}(o_i|q)}, 1 - \varepsilon, 1 + \varepsilon \right) \hat{A}_i \right) - \beta \cdot D_{\text{KL}}(\pi_{\theta} \| \pi_{\text{ref}}) \right], \quad (3)$$

where ε and β are hyperparameters controlling the clipping range and KL regularization strength, respectively. π_{ref} denotes the reference policy model. The normalized advantage term is given by $\hat{A}_i = \frac{r_i - \text{mean}(\mathbf{r})}{\text{std}(\mathbf{r})}$, providing a normalized signal that facilitates stable and efficient policy updates.

The reward mechanism in RL Binding focuses on motion similarity and semantic alignment, ensuring that generated motions are temporally coherent and semantically faithful to the textual input. A format reward is also included to maintain structural validity, collectively enabling effective reinforcement learning without costly human annotations.

Format Reward. To ensure that the content generated by the model has a resolvable structure, we introduce Format Reward r_{format} . This reward detects through regularization expressions whether the generated results strictly follow the predefined format:

`<think>{Decomposed CoT}</think><Motion>{Motion tokens}</Motion>.`

Here, curly braces and their enclosed content denote placeholders, representing the generated CoT and the corresponding motion tokens, respectively. If the generated content exactly matches this required format, we assign a reward of 1. Otherwise, the reward is set to 0.

Motion Similarity Reward. To enforce temporal and spatial consistency, RL Binding computes a motion similarity reward r_{motion} between the generated motion $\hat{\mathbf{m}}$ and the ground-truth motion \mathbf{m} . A pre-trained motion encoder f_{motion} Guo et al. (2022a) is used to extract feature embeddings, and the reward is defined as the cosine similarity between these embeddings:

$$r_{\text{motion}} = \frac{f_{\text{motion}}(\hat{\mathbf{m}}) \cdot f_{\text{motion}}(\mathbf{m})}{\|f_{\text{motion}}(\hat{\mathbf{m}})\|_2 \cdot \|f_{\text{motion}}(\mathbf{m})\|_2} \quad (4)$$

Semantic Similarity Reward. To ensure that the generated motion semantically corresponds to the input textual description T , RL binding evaluates the semantic similarity reward r_{semantic} , which measures the alignment between the motion embedding and the language embedding in a shared latent space. Both embeddings are extracted using pre-trained encoders f_{motion} and f_{text} , respectively (also from Guo et al. (2022a)). The reward is defined as:

$$r_{\text{semantic}} = \frac{f_{\text{motion}}(\hat{\mathbf{m}}) \cdot f_{\text{text}}(T)}{\|f_{\text{motion}}(\hat{\mathbf{m}})\|_2 \cdot \|f_{\text{text}}(T)\|_2} \quad (5)$$

These rewards are integrated into GRPO via groupwise preference ranking, enabling RL Binding to simultaneously enforce motion realism and semantic fidelity.

4 EXPERIMENTS

4.1 EXPERIMENTAL SETTINGS

Datasets We evaluate our method on two widely-used benchmarks: **HumanML3D** Guo et al. (2022a), **KIT-ML** Plappert et al. (2016) and **BABEL** Punnakkal et al. (2021). HumanML3D contains 14, 616 motions and 44, 970 textual descriptions, sourced AMASS Mahmood et al. (2019) and

Table 1: **Quantitative results of Motion-R1 on HumanML3D Guo et al. (2022a) and KIT-ML Plappert et al. (2016).** The evaluations are conducted 20 times to obtain a 95% confidence interval. Best results are highlighted in **bold** and the second best in underline.

Methods	R-Precision \uparrow			FID \downarrow	MM-Dist \downarrow	Diversity \uparrow	MModality \uparrow
	Top 1	Top 2	Top 3				
HumanML3D							
MDM (Tevet et al., 2023)	0.320 \pm .005	0.498 \pm .004	0.611 \pm .007	0.544 \pm .044	5.566 \pm .027	9.559 \pm .086	2.799 \pm .072
MLD (Chen et al., 2023)	0.481 \pm .003	0.673 \pm .003	0.772 \pm .002	0.473 \pm .013	3.196 \pm .010	9.724 \pm .082	2.413 \pm .079
MotionDiffuse (Zhang et al., 2022a)	0.491 \pm .001	0.681 \pm .001	0.782 \pm .001	0.630 \pm .001	3.113 \pm .001	9.410 \pm .049	1.553 \pm .042
T2M (Guo et al., 2022a)	0.457 \pm .002	0.559 \pm .007	0.740 \pm .003	1.067 \pm .002	3.340 \pm .008	9.188 \pm .002	2.090 \pm .083
TM2T (Guo et al., 2022b)	0.424 \pm .003	0.618 \pm .003	0.729 \pm .002	1.501 \pm .017	3.467 \pm .011	8.589 \pm .076	<u>2.424</u> \pm .093
T2M-GPT (Zhang et al., 2023a)	0.491 \pm .003	0.680 \pm .003	0.775 \pm .002	<u>0.116</u> \pm .004	3.118 \pm .011	9.761 \pm .081	1.856 \pm .011
MotionGPT (Jiang et al., 2023)	0.492 \pm .003	0.681 \pm .003	0.778 \pm .002	0.232 \pm .008	3.096 \pm .008	9.528 \pm .071	2.008 \pm .084
MoMask Guo et al. (2024)	0.521 \pm .002	<u>0.713</u> \pm .002	<u>0.807</u> \pm .002	0.045 \pm .002	<u>2.958</u> \pm .008	9.620 \pm .064	1.241 \pm .040
MotionChain (Jiang et al., 2024)	0.504 \pm .003	0.617 \pm .002	0.790 \pm .003	0.248 \pm .009	3.033 \pm .010	9.470 \pm .075	1.727 \pm .014
MotionLLM Wu et al. (2024)	0.515 \pm .004	0.691 \pm .003	0.801 \pm .004	0.230 \pm .009	2.967 \pm .020	<u>9.908</u> \pm .102	2.142 \pm .014
MotionGPT-2 Wang et al. (2024)	0.496 \pm .002	0.691 \pm .003	0.782 \pm .004	0.191 \pm .004	3.080 \pm .013	9.860 \pm .026	2.137 \pm .022
Motion-R1	<u>0.515</u> \pm .003	0.719 \pm .002	0.818 \pm .002	0.201 \pm .004	2.854 \pm .010	10.026 \pm .075	2.317 \pm .105
KIT-ML							
TM2T (Guo et al., 2022b)	0.280 \pm .005	0.463 \pm .006	0.587 \pm .005	3.599 \pm .153	4.591 \pm .026	9.473 \pm .117	3.292 \pm .081
T2M (Guo et al., 2022a)	0.361 \pm .006	0.559 \pm .007	0.681 \pm .007	3.022 \pm .107	3.488 \pm .028	10.720 \pm .143	2.052 \pm .107
MDM (Tevet et al., 2023)	0.164 \pm .004	0.291 \pm .004	0.396 \pm .004	<u>0.497</u> \pm .021	9.191 \pm .022	10.850 \pm .109	1.907 \pm .214
MotionDiffuse (Zhang et al., 2022a)	<u>0.417</u> \pm .004	0.621 \pm .004	0.739 \pm .004	1.954 \pm .062	<u>2.958</u> \pm .005	<u>11.100</u> \pm .143	0.730 \pm .013
MLD (Chen et al., 2023)	0.390 \pm .008	0.609 \pm .008	0.734 \pm .007	0.404 \pm .027	3.204 \pm .027	10.800 \pm .117	2.192 \pm .071
T2M-GPT (Zhang et al., 2023a)	0.416 \pm .006	0.627 \pm .006	0.745 \pm .006	0.514 \pm .029	3.007 \pm .023	10.920 \pm .108	1.570 \pm .039
AttT2M Zhong et al. (2023)	0.413 \pm .005	<u>0.632</u> \pm .006	<u>0.751</u> \pm .006	0.870 \pm .039	3.039 \pm .021	10.960 \pm .123	<u>2.281</u> \pm .047
MotionLLM Wu et al. (2024)	0.409 \pm .006	0.624 \pm .007	0.750 \pm .005	0.781 \pm .026	2.982 \pm .022	11.407 \pm .103	—
Motion-R1	0.431 \pm .003	0.638 \pm .002	0.761 \pm .003	0.287 \pm .004	3.196 \pm .040	10.875 \pm .052	2.262 \pm .014

HumanAct12 Guo et al. (2020). KIT-ML includes 3,911 motion clips and 6,278 descriptions, derived from KIT Mandery et al. (2015) and CMU CMU Graphics Lab datasets. BABEL provides over 43 hours of motion capture sequences with 28k sequence-level and 63k frame-level action annotations from AMASS Mahmood et al. (2019).

Evaluation Metrics Following standard protocols Guo et al. (2022a); Zhang et al. (2023a); Wu et al. (2024), we report R-Precision@1/2/3, FID, Diversity, MM-Dist, and MModality. These metrics respectively evaluate retrieval accuracy, distributional realism, sample diversity, text-motion alignment, and one-to-many generation ability.

Implementation Details We utilize DeepSeek-R1 Guo et al. (2025) to generate structured reasoning traces for complex motion descriptions, serving as intermediate representations that bridge textual prompts and motion tokens. Within Motion-R1, we adopt Qwen-2.5-3B-Instruct Team (2024) as the backbone model for its strong multi-step reasoning and efficient size, facilitating stable RL training. The generated CoTs condition motion synthesis and provide targets for GRPO optimization. Experiments are conducted on NVIDIA H20 GPUs. Additional experimental details are provided in Appendix A.3.

4.2 QUANTITATIVE EVALUATION

We evaluate the performance of Motion-R1 on HumanML3D and KIT-ML datasets, comparing it with state-of-the-art methods, ranging from VAE-based to diffusion-based models. For the diffusion-based model, we select MDM Tevet et al. (2023), MLD Chen et al. (2023), MotionDiffuse Zhang et al. (2022a). For the VAE-based model, we choose T2M Guo et al. (2022a), TM2T Guo et al. (2022b), T2M-GPT Zhang et al. (2023a), MotionGPT Jiang et al. (2023), MoMask Guo et al. (2024), MotionChain Jiang et al. (2024), MotionLLM Wu et al. (2024) and MotionGPT-2 Wang et al. (2024).

We follow the same evaluation settings as prior work Guo et al. (2022a); Wu et al. (2024) and the BABEL setup from Zhuo et al. (2024). Quantitative results on HumanML3D and KIT-ML are shown in Table 1. Results on BABEL are provided in the Appendix A.4.

On **HumanML3D**, Motion-R1 attains strong and balanced performance across semantic and motion-quality metrics. It achieves R-Precision@1/2/3 = **0.515 / 0.719 / 0.818**, with the latter two values being the best in the table and R-Precision@1 at near-top level. In terms of realism, Motion-R1 yields a competitive FID of **0.201**, comparable to recent strong baselines (e.g., MotionGPT-2:

0.191, MotionGPT: 0.232). Motion-R1 also attains the lowest MM-Dist (**2.854**), indicating superior alignment in the joint motion–language embedding space, and the highest Diversity score (**10.026**), suggesting better modeling of the one-to-many nature of text-to-motion. Its MModality score (**2.317**) is likewise competitive with top methods. Together, these results indicate that the combination of decomposed CoT supervision and RL Binding yields motions that are both semantically aligned and high-fidelity.

On **KIT-ML**, Motion-R1 consistently leads the comparators on retrieval and fidelity metrics: R-Precision@1/2/3 = **0.431 / 0.638 / 0.761** (all best), and FID = **0.287** (best). While MM-Dist (3.196) is not the lowest in the table, Motion-R1 maintains strong Diversity (**10.875**) and solid MModality (**2.262**), demonstrating robust generalization across a dataset with different statistics. Overall, Motion-R1 provides a favorable trade-off between semantic alignment, motion realism, and diversity on both benchmarks, empirically supporting the effectiveness of the Decomposed CoT Data Engine and RL Binding.

4.3 QUALITATIVE ANALYSIS AND VISUALIZATION

To complement the quantitative evaluation, we provide qualitative comparisons between Motion-R1 and existing state-of-the-art methods. We divide this section into two parts: (1) in-distribution prompts from standard benchmarks, and (2) out-of-distribution instructions that require compositional reasoning and generalization. These visualizations highlight the advantages of Motion-R1 in producing semantically coherent, diverse, and controllable motion sequences. Note that more visualizations are provided in supplementary video.

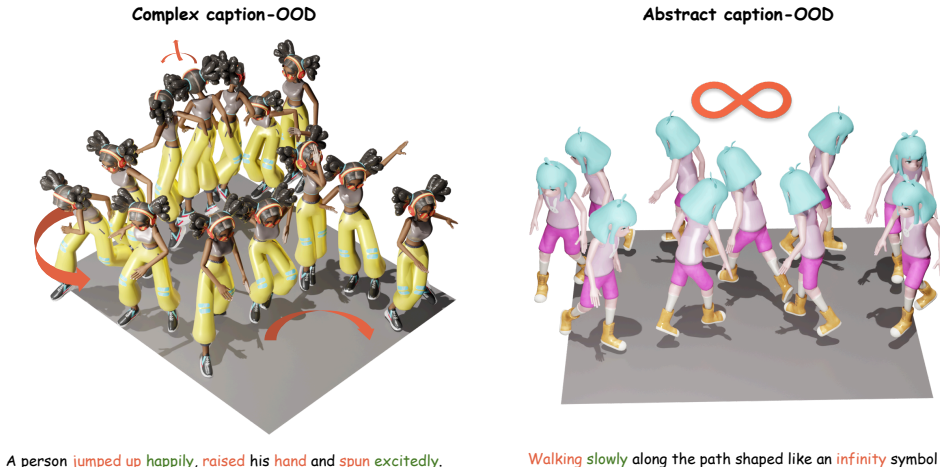


Figure 4: **Motion-R1 results on out-of-distribution prompts.** Left: Complex caption with multi-step reasoning. Right: Abstract caption requiring semantic understanding.

In-Distribution Visualization. We visualize results and compare Motion-R1 with MotionLLM as shown in Figure 3 (left). Motion-R1 generates smooth, coherent sequences that respect spatial and temporal semantics — for example, producing a continuous circular walk with natural timing, while MotionLLM Wu et al. (2024) often fails to complete the circle or exhibits abrupt stops.

Out-of-Distribution Visualization. To evaluate generalization, we show two out-of-distribution prompts in Figure 3 (middle, right). For “After hearing a loud noise...”, Motion-R1 clearly separates reaction, retreat, and re-approach; MotionLLM merges steps or omits gestures. For “A person is serving in badminton,” Motion-R1 produces a plausible serve motion with arm lift and forward strike, while MotionLLM generates generic or repetitive movements. More examples in Figure 4 further demonstrate Motion-R1’s ability to interpret abstract instructions and maintain temporal coherence. All results are generated without post-processing.

These examples show that Motion-R1 generalizes well to unseen instructions through explicit CoT-style reasoning, whereas baseline methods struggle with long-horizon dependencies and abstract

actions. To further validate these observations from a human perspective, we conducted a user study evaluating semantic consistency and motion fluency. As detailed in Appendix A.5, our method was significantly preferred by users over state-of-the-art baselines, confirming its superior perceptual quality.

4.4 ABLATION STUDY

To assess the contribution of each component in our framework, we conduct an ablation study on the HumanML3D dataset, as shown in Table 2. Specifically, we evaluate the impact of three key components: Decomposed CoT Data Engine and RL Binding (the semantic similarity reward (R_{sem}), and the motion similarity reward (R_{motion})).

All ablated variants achieve comparable performance, showing the robustness of our design. Using the Decomposed CoT Data Engine alone yields the weakest results (R-Precision Top-1: $0.340 \pm .002$, FID: $0.530 \pm .015$), while adding either R_{sem} or R_{motion} significantly improves alignment (Top-1: $0.483 \pm .002$, FID: $0.281 \pm .008$).

With all components combined, the model reaches the best or second-best performance across most metrics, including the lowest FID (**$0.201 \pm .004$**) and highest Diversity (**$10.026 \pm .075$**). These results confirm the complementary roles of structured reasoning and semantic/motion-level rewards in producing diverse, semantically faithful, and high-quality motion.

Table 2: **Ablation study on HumanML3D Guo et al. (2022a)**. CoT, R_{sem} , and R_{motion} denote Decomposed CoT Data Engine, the semantic similarity reward, and the motion similarity reward, respectively, with additional columns showing effects of self-verification mechanism and LLM choice for Decomposed CoT Data Engine. Best results are highlighted in **bold** and the second best in underline.

CoT	R_{sem}	R_{motion}	Verification	CoT LLM	R Precision \uparrow			FID \downarrow	MM-Dist \downarrow	Diversity \uparrow	MModality \uparrow
					Top 1	Top 2	Top 3				
\checkmark			\checkmark	Deepseek-R1	$0.340 \pm .002$	$0.503 \pm .002$	$0.603 \pm .002$	$0.530 \pm .015$	$4.216 \pm .015$	$9.696 \pm .090$	$4.762 \pm .249$
\checkmark	\checkmark		\checkmark	Deepseek-R1	$0.482 \pm .002$	$0.690 \pm .003$	$0.799 \pm .001$	$0.297 \pm .004$	$2.963 \pm .004$	$9.537 \pm .021$	$2.317 \pm .015$
\checkmark		\checkmark	\checkmark	Deepseek-R1	$0.483 \pm .002$	$0.690 \pm .002$	$0.799 \pm .002$	$0.281 \pm .008$	$2.947 \pm .007$	$9.848 \pm .082$	$1.903 \pm .276$
\checkmark	\checkmark	\checkmark		Deepseek-R1	$0.489 \pm .002$	$0.688 \pm .003$	$0.764 \pm .002$	$0.234 \pm .003$	$3.127 \pm .012$	$9.785 \pm .084$	$2.408 \pm .078$
\checkmark	\checkmark	\checkmark	\checkmark	GPT-4o	$0.520 \pm .002$	$0.709 \pm .003$	<u>$0.812 \pm .003$</u>	<u>$0.213 \pm .009$</u>	<u>$2.895 \pm .011$</u>	<u>$9.963 \pm .063$</u>	$2.445 \pm .094$
	\checkmark			-	$0.322 \pm .002$	$0.497 \pm .003$	$0.610 \pm .002$	$1.705 \pm .034$	$4.206 \pm .010$	$9.914 \pm .057$	<u>$4.194 \pm .192$</u>
		\checkmark		-	$0.365 \pm .002$	$0.526 \pm .001$	$0.627 \pm .003$	$0.766 \pm .021$	$4.136 \pm .005$	$9.711 \pm .041$	$4.067 \pm .200$
	\checkmark	\checkmark		-	$0.365 \pm .002$	$0.539 \pm .003$	$0.644 \pm .002$	$1.656 \pm .015$	$4.024 \pm .012$	$9.720 \pm .024$	$4.008 \pm .119$
\checkmark	\checkmark	\checkmark	\checkmark	Deepseek-R1	<u>$0.515 \pm .003$</u>	$0.719 \pm .002$	$0.818 \pm .002$	$0.201 \pm .004$	$2.854 \pm .010$	$10.026 \pm .075$	$2.317 \pm .105$

We also examine the effects of self-verification mechanism and different LLM choices for Decomposed CoT Data Engine. For self-verification mechanism, Manual evaluation of approximately 500 randomly sampled data points from the HumanML3D dataset reveals that the initial error rate in decomposed CoT generation is around 20%, primarily due to format violations, hallucinations, redundant steps and repetitions. After self-verification, the error rate decreases to approximately 3%. The ablation results show that without self-verification, performance drops significantly, while self-verification restores optimal performance. Regarding LLM choices, experiment using GPT-4o Hurst et al. (2024) shows competitive results compared to Deepseek-R1 Guo et al. (2025), confirming that our framework’s effectiveness stems from the overall design rather than dependency on particular model selections.

5 CONCLUSION

In this work, we introduced **Motion-R1**, a unified framework for text-to-motion generation that integrates a Decomposed CoT Data Engine and RL Binding. The Decomposed CoT Data Engine generates structured, step-by-step reasoning traces to decompose complex language into interpretable action plans, while RL Binding optimizes motion synthesis through GRPO with semantic and motion-level reward alignment. Together, these innovations enable coherent, semantically faithful, and high-quality motion generation without relying on costly human annotations, improving controllability, diversity, and generalization.

6 ETHICS STATEMENT

This work introduces Motion-R1, a framework for text-to-motion generation. While the method enables high-fidelity and semantically aligned motion synthesis, it shares general risks associated with generative models, including the potential misuse for creating misleading, unsafe, or inappropriate motion sequences. We strongly discourage such applications and emphasize that Motion-R1 is intended strictly for research, educational, and other socially beneficial purposes. Users should exercise caution, ensure compliance with ethical guidelines, and consider privacy and consent when applying the model to real-world scenarios.

7 REPRODUCIBILITY STATEMENT

We are committed to ensuring the reproducibility of our work. Details of the framework, training protocols, and hyperparameters are provided in Section 3, Subsection 4.1 and Appendix A.2; A.3. Code for our method will be made publicly available to support replication and future research.

REFERENCES

- Josh Achiam, Steven Adler, Sandhini Agarwal, Lama Ahmad, Ilge Akkaya, Florencia Leoni Aleman, Diogo Almeida, Janko Altmenschmidt, Sam Altman, Shyamal Anadkat, et al. Gpt-4 technical report. *arXiv preprint arXiv:2303.08774*, 2023.
- Hyemin Ahn, Timothy Ha, Yunho Choi, Hwiyeon Yoo, and Songhwai Oh. Text2action: Generative adversarial synthesis from language to action, 2017.
- Chaitanya Ahuja and Louis-Philippe Morency. Language2pose: Natural language grounded pose forecasting, 2019.
- Nikos Athanasiou, Mathis Petrovich, Michael J. Black, and Gül Varol. Teach: Temporal action composition for 3d humans, 2022.
- Pratyay Banerjee, Tejas Gokhale, Yezhou Yang, and Chitta Baral. Weakly supervised relative spatial reasoning for visual question answering. In *Proceedings of the IEEE/CVF International Conference on Computer Vision*, pp. 1908–1918, 2021.
- Xin Chen, Biao Jiang, Wen Liu, Zilong Huang, Bin Fu, Tao Chen, Jingyi Yu, and Gang Yu. Executing your commands via motion diffusion in latent space, 2023.
- CMU Graphics Lab. CMU Graphics Lab Motion Capture Database. <http://mocap.cs.cmu.edu/>.
- Rishabh Dabral, Muhammad Hamza Mughal, Vladislav Golyanik, and Christian Theobalt. Mofusion: A framework for denoising-diffusion-based motion synthesis, 2023.
- Anindita Ghosh, Noshaba Cheema, Cennet Oguz, Christian Theobalt, and Philipp Slusallek. Synthesis of compositional animations from textual descriptions, 2023.
- Ian J Goodfellow, Jean Pouget-Abadie, Mehdi Mirza, Bing Xu, David Warde-Farley, Sherjil Ozair, Aaron Courville, and Yoshua Bengio. Generative adversarial nets. *Advances in neural information processing systems*, 27, 2014.
- Chuan Guo, Xinxin Zuo, Sen Wang, Shihao Zou, Qingyao Sun, Annan Deng, Minglun Gong, and Li Cheng. Action2motion: Conditioned generation of 3d human motions. In *Proceedings of the 28th ACM International Conference on Multimedia*, pp. 2021–2029, 2020.
- Chuan Guo, Shihao Zou, Xinxin Zuo, Sen Wang, Wei Ji, Xingyu Li, and Li Cheng. Generating diverse and natural 3d human motions from text. In *Proceedings of the IEEE/CVF Conference on Computer Vision and Pattern Recognition (CVPR)*, pp. 5152–5161, June 2022a.
- Chuan Guo, Xinxin Zuo, Sen Wang, and Li Cheng. Tm2t: Stochastic and tokenized modeling for the reciprocal generation of 3d human motions and texts, 2022b.

- Chuan Guo, Yuxuan Mu, Muhammad Gohar Javed, Sen Wang, and Li Cheng. Momask: Generative masked modeling of 3d human motions. In *Proceedings of the IEEE/CVF Conference on Computer Vision and Pattern Recognition*, pp. 1900–1910, 2024.
- Daya Guo, Dejian Yang, Haowei Zhang, Junxiao Song, Ruoyu Zhang, Runxin Xu, Qihao Zhu, Shirong Ma, Peiyi Wang, Xiao Bi, et al. Deepseek-r1: Incentivizing reasoning capability in llms via reinforcement learning. *arXiv preprint arXiv:2501.12948*, 2025.
- Wen Guo, Yuming Du, Xi Shen, Vincent Lepetit, Xavier Alameda-Pineda, and Francesc Moreno-Noguer. Back to mlp: A simple baseline for human motion prediction, 2022c.
- Gaoge Han, Mingjiang Liang, Jinglei Tang, Yongkang Cheng, Wei Liu, and Shaoli Huang. Reindiffuse: Crafting physically plausible motions with reinforced diffusion model, 2024a. URL <https://arxiv.org/abs/2410.07296>.
- Haonan Han, Xiangzuo Wu, Huan Liao, Zunnan Xu, Zhongyuan Hu, Ronghui Li, Yachao Zhang, and Xiu Li. Atom: Aligning text-to-motion model at event-level with gpt-4vision reward, 2024b. URL <https://arxiv.org/abs/2411.18654>.
- Wentao Zhu Haoru Wang, Yishu Xu Luyi Miao, Qi Tian Feng Gao, and Yizhou Wang. Aligning human motion generation with human perceptions, 2025. URL <https://arxiv.org/abs/2407.02272>.
- Jonathan Ho, Ajay Jain, and Pieter Abbeel. Denoising diffusion probabilistic models. *arXiv preprint arXiv:2006.11239*, 2020.
- Fangzhou Hong, Mingyuan Zhang, Liang Pan, Zhongang Cai, Lei Yang, and Ziwei Liu. Avatarclip: Zero-shot text-driven generation and animation of 3d avatars, 2022.
- Aaron Hurst, Adam Lerer, Adam P Goucher, Adam Perelman, Aditya Ramesh, Aidan Clark, AJ Ostrow, Akila Welihinda, Alan Hayes, Alec Radford, et al. Gpt-4o system card. *arXiv preprint arXiv:2410.21276*, 2024.
- Biao Jiang, Xin Chen, Wen Liu, Jingyi Yu, Gang Yu, and Tao Chen. Motiongpt: Human motion as a foreign language, 2023.
- Biao Jiang, Xin Chen, Chi Zhang, Fukun Yin, Zhuoyuan Li, Gang YU, and Jiayuan Fan. Motion-chain: Conversational motion controllers via multimodal prompts, 2024.
- Leslie Pack Kaelbling, Michael L Littman, and Andrew W Moore. Reinforcement learning: A survey. *Journal of artificial intelligence research*, 4:237–285, 1996.
- Jihoon Kim, Jiseob Kim, and Sungjoon Choi. Flame: Free-form language-based motion synthesis & editing, 2023.
- Jing Yu Koh, Daniel Fried, and Russ R Salakhutdinov. Generating images with multimodal language models. *Advances in Neural Information Processing Systems*, 36:21487–21506, 2023.
- Junnan Li, Dongxu Li, Silvio Savarese, and Steven Hoi. Blip-2: Bootstrapping language-image pre-training with frozen image encoders and large language models. In *International conference on machine learning*, pp. 19730–19742. PMLR, 2023.
- Zhengdao Li, Siheng Wang, Zeyu Zhang, and Hao Tang. Remomask: Retrieval-augmented masked motion generation. *arXiv preprint arXiv:2508.02605*, 2025.
- Xiaoyang Liu, Yunyao Mao, Wengang Zhou, and Houqiang Li. Motionrl: Align text-to-motion generation to human preferences with multi-reward reinforcement learning, 2024. URL <https://openreview.net/forum?id=v1oQ0kNq0w>.
- Yuqi Liu, Bohao Peng, Zhisheng Zhong, Zihao Yue, Fanbin Lu, Bei Yu, and Jiaya Jia. Seg-zero: Reasoning-chain guided segmentation via cognitive reinforcement. *arXiv preprint arXiv:2503.06520*, 2025.

- Naureen Mahmood, Nima Ghorbani, Nikolaus F. Troje, Gerard Pons-Moll, and Michael J. Black. AMASS: Archive of motion capture as surface shapes. In *International Conference on Computer Vision*, pp. 5442–5451, October 2019.
- Christian Mandery, Ömer Terlemez, Martin Do, Nikolaus Vahrenkamp, and Tamim Asfour. The kit whole-body human motion database. In *2015 International Conference on Advanced Robotics (ICAR)*, pp. 329–336, 2015. doi: 10.1109/ICAR.2015.7251476.
- Yunyao Mao, Xiaoyang Liu, Wengang Zhou, Zhenbo Lu, and Houqiang Li. Learning generalizable human motion generator with reinforcement learning, 2024. URL <https://arxiv.org/abs/2405.15541>.
- Jiazhen Pan, Che Liu, Junde Wu, Fenglin Liu, Jiayuan Zhu, Hongwei Bran Li, Chen Chen, Cheng Ouyang, and Daniel Rueckert. Medvlm-r1: Incentivizing medical reasoning capability of vision-language models (vlms) via reinforcement learning. *arXiv preprint arXiv:2502.19634*, 2025.
- Mathis Petrovich, Michael J. Black, and Gül Varol. Temos: Generating diverse human motions from textual descriptions, July 2022.
- Matthias Plappert, Christian Mandery, and Tamim Asfour. The kit motion-language dataset. *Big Data*, 4(4):236–252, 2016. ISSN 2167-6461, 2167-647X. doi: 10.1089/big.2016.0028.
- Abhinanda R. Punnakkal, Arjun Chandrasekaran, Nikos Athanasiou, Alejandra Quiros-Ramirez, and Michael J. Black. BABEL: Bodies, action and behavior with english labels. In *Proceedings IEEE/CVF Conf. on Computer Vision and Pattern Recognition (CVPR)*, pp. 722–731, June 2021.
- John Schulman, Filip Wolski, Prafulla Dhariwal, Alec Radford, and Oleg Klimov. Proximal policy optimization algorithms. *arXiv preprint arXiv:1707.06347*, 2017.
- Yonatan Shafir, Guy Tevet, Roy Kapon, and Amit H Bermano. Human motion diffusion as a generative prior. *arXiv preprint arXiv:2303.01418*, 2023.
- Zhihong Shao, Peiyi Wang, Qihao Zhu, Runxin Xu, Junxiao Song, Xiao Bi, Haowei Zhang, Mingchuan Zhang, Y. K. Li, Y. Wu, and Daya Guo. Deepseekmath: Pushing the limits of mathematical reasoning in open language models, 2024. URL <https://arxiv.org/abs/2402.03300>.
- Huajie Tan, Yuheng Ji, Xiaoshuai Hao, Minglan Lin, Pengwei Wang, Zhongyuan Wang, and Shanghang Zhang. Reason-rft: Reinforcement fine-tuning for visual reasoning. *arXiv preprint arXiv:2503.20752*, 2025.
- Yunlong Tang, Jing Bi, Siting Xu, Luchuan Song, Susan Liang, Teng Wang, Daoan Zhang, Jie An, Jingyang Lin, Rongyi Zhu, et al. Video understanding with large language models: A survey. *IEEE Transactions on Circuits and Systems for Video Technology*, 2025.
- Qwen Team. Qwen2.5: A party of foundation models, September 2024. URL <https://qwenlm.github.io/blog/qwen2.5/>.
- Guy Tevet, Brian Gordon, Amir Hertz, Amit H Bermano, and Daniel Cohen-Or. Motionclip: Exposing human motion generation to clip space. *arXiv preprint arXiv:2203.08063*, 2022.
- Guy Tevet, Sigal Raab, Brian Gordon, Yoni Shafir, Daniel Cohen-or, and Amit Haim Bermano. Human motion diffusion model. In *The Eleventh International Conference on Learning Representations*, 2023. URL <https://openreview.net/forum?id=SJ1kSyO2jwu>.
- Yuan Wang, Di Huang, Yaqi Zhang, Wanli Ouyang, Jile Jiao, Xuetao Feng, Yan Zhou, Pengfei Wan, Shixiang Tang, and Dan Xu. Motiongpt-2: A general-purpose motion-language model for motion generation and understanding, 2024.
- Jason Wei, Xuezhi Wang, Dale Schuurmans, Maarten Bosma, Brian Ichter, Fei Xia, Ed H. Chi, Quoc V. Le, and Denny Zhou. Chain-of-thought prompting elicits reasoning in large language models. In *NeurIPS*, 2022.

- Jiayang Wu, Wensheng Gan, Zefeng Chen, Shicheng Wan, and Philip S Yu. Multimodal large language models: A survey. In *2023 IEEE International Conference on Big Data (BigData)*, pp. 2247–2256. IEEE, 2023.
- Qi Wu, Yubo Zhao, Yifan Wang, Xinhang Liu, Yu-Wing Tai, and Chi-Keung Tang. Motion-agent: A conversational framework for human motion generation with llms. *arXiv preprint arXiv:2405.17013*, 2024.
- Siheng Xiong, Yuan Yang, Ali Payani, James C Kerce, and Faramarz Fekri. Teilp: Time prediction over knowledge graphs via logical reasoning, 2024. URL <https://arxiv.org/abs/2312.15816>.
- Guowei Xu, Peng Jin, Hao Li, Yibing Song, Lichao Sun, and Li Yuan. LLaVA-CoT: Let Vision Language Models Reason Step-by-Step, 2025.
- Junpeng Yue, Zepeng Wang, Yuxuan Wang, Weishuai Zeng, Jiangxing Wang, Xinrun Xu, Yu Zhang, Sipeng Zheng, Ziluo Ding, and Zongqing Lu. RL from physical feedback: Aligning large motion models with humanoid control, 2025. URL <https://arxiv.org/abs/2506.12769>.
- Jianrong Zhang, Yangsong Zhang, Xiaodong Cun, Yong Zhang, Hongwei Zhao, Hongtao Lu, Xi Shen, and Ying Shan. Generating human motion from textual descriptions with discrete representations. In *Proceedings of the IEEE/CVF conference on computer vision and pattern recognition*, pp. 14730–14740, 2023a.
- Mingyuan Zhang, Zhongang Cai, Liang Pan, Fangzhou Hong, Xinying Guo, Lei Yang, and Ziwei Liu. Motiondiffuse: Text-driven human motion generation with diffusion model. *arXiv preprint arXiv:2208.15001*, 2022a.
- Mingyuan Zhang, Zhongang Cai, Liang Pan, Fangzhou Hong, Xinying Guo, Lei Yang, and Ziwei Liu. Motiondiffuse: Text-driven human motion generation with diffusion model, 2022b.
- Qinsheng Zhang, Jiaming Song, Xun Huang, Yongxin Chen, and Ming-Yu Liu. Diffcollage: Parallel generation of large content with diffusion models. In *2023 IEEE/CVF Conference on Computer Vision and Pattern Recognition (CVPR)*, pp. 10188–10198. IEEE, 2023b.
- Zeyu Zhang, Hang Gao, Akide Liu, Qi Chen, Feng Chen, Yiran Wang, Danning Li, Rui Zhao, Zhenming Li, Zhongwen Zhou, et al. Kmm: Key frame mask mamba for extended motion generation. *arXiv preprint arXiv:2411.06481*, 2024a.
- Zeyu Zhang, Akide Liu, Qi Chen, Feng Chen, Ian Reid, Richard Hartley, Bohan Zhuang, and Hao Tang. Infinimotion: Mamba boosts memory in transformer for arbitrary long motion generation. *arXiv preprint arXiv:2407.10061*, 2024b.
- Zeyu Zhang, Akide Liu, Ian Reid, Richard Hartley, Bohan Zhuang, and Hao Tang. Motion mamba: Efficient and long sequence motion generation. In *European Conference on Computer Vision*, pp. 265–282. Springer, 2024c.
- Zeyu Zhang, Yiran Wang, Biao Wu, Shuo Chen, Zhiyuan Zhang, Shiya Huang, Wenbo Zhang, Meng Fang, Ling Chen, and Yang Zhao. Motion avatar: Generate human and animal avatars with arbitrary motion. *arXiv preprint arXiv:2405.11286*, 2024d.
- Zeyu Zhang, Yiran Wang, Danning Li, Dong Gong, Ian Reid, and Richard Hartley. Flashmo: Geometric interpolants and frequency-aware sparsity for scalable efficient motion generation. In *The Thirty-ninth Annual Conference on Neural Information Processing Systems*, 2025a.
- Zeyu Zhang, Yiran Wang, Wei Mao, Danning Li, Rui Zhao, Biao Wu, Zirui Song, Bohan Zhuang, Ian Reid, and Richard Hartley. Motion anything: Any to motion generation. *arXiv preprint arXiv:2503.06955*, 2025b.
- Chongyang Zhong, Lei Hu, Zihao Zhang, and Shihong Xia. Attt2m: Text-driven human motion generation with multi-perspective attention mechanism. In *Proceedings of the IEEE/CVF international conference on computer vision*, pp. 509–519, 2023.

Zixiang Zhou and Baoyuan Wang. Ude: A unified driving engine for human motion generation, 2022.

Wenjie Zhuo, Fan Ma, and Hehe Fan. Infinidreamer: Arbitrarily long human motion generation via segment score distillation. *arXiv preprint arXiv:2411.18303*, 2024.

A APPENDIX

A.1 STATEMENT ON THE USE OF LLM

Large Language Models (ChatGPT by OpenAI) were used exclusively to improve the clarity and fluency of English writing. They were not involved in research ideation, experimental design, data analysis, or interpretation. The authors take full responsibility for all content.

A.2 DETAILS OF PROMPT

To enable reasoning-aware motion generation, we design three distinct types of prompts that correspond to different training phases and supervision signals. These prompts guide the LLM during both supervised and reinforcement learning stages in a progressively structured manner.

A.2.1 DECOMPOSED CoT DATA ENGINE

The following prompt is used in the Decomposed CoT Data Engine, which encourages the language model to generate structured reasoning traces and explicit motion planning steps based on free-form motion descriptions.

```

You are an assistant who helps users understand descriptions
of human motions. The user begins by describing the motion
they envision, and you help break that description down into
a few simple descriptions of the action and show the thought
process.
## Instruction:
1. User-Provided Description: The user's description may
include both straightforward and abstract descriptions of
human motion, such as "A person ties their shoelaces" or "A
person waves goodbye."
2. Reasoning process: For each human motion description, you
first think about the reasoning process in the mind to decide
how to break down the description into simple, atomic motions.
Ensure that each atomic motion is independent and focuses
on a straightforward, non-elaborate motion description. If
user's description is already simple and atomic, you don't
need to break it down. Show your work in <think> </think>
tags. Think step by step inside <think> tags. Then generate
motions matching the atomic motion descriptions.
## Response Format:
Your response should include a step-by-step thinking process:
<think>...</think>
## Examples:
### Example 1:
- User: "a person waves goodbye."
- Assistant:
<think> The user wants me to break down the action "a person
waves goodbye" into simpler steps if necessary. Waving
goodbye is already a fairly atomic action, as it describes a
single, recognizable motion.
Therefore, the correct response would be:
1. wave hand.
</think>

```

Example 2:

- User: "a person ties their shoelaces and stands up."

- Assistant:

<think> The user wants me to break down the description "a person ties their shoelaces and stands up" into simple steps. First, I need to visualize tying shoelaces: it involves bending down, grabbing the laces, tying them, and then standing up. Since "tie shoelaces" can be kept as a single action for simplicity, I'll treat that as one step. Then comes standing up.

Let me ensure temporal and logical order: first bend down and tie, then stand up. Each step is independent and physically distinct.

Therefore, the correct response would be:

1. bend down and tie shoelaces.
2. stand up.

</think>

Example 3:

- User: "a person opens a door and enters the room."

- Assistant:

<think> The user wants me to simplify the motion "a person opens a door and enters the room." This involves first manipulating the door, then walking through the doorway. I should break this into: (1) reach and grasp the doorknob, (2) pull or push the door, (3) walk forward through the doorway. Check that each is a simple motor action. Yes, these three steps should be clear and sequential.

Therefore, the correct response would be:

1. reach and grasp the doorknob.
2. open the door.
3. walk forward through the doorway.

</think>

A.2.2 MOTION-R1

Used in the final training stage, this unified format integrates both reasoning and motion generation to reinforce semantic decomposition and executable token prediction jointly.

You are an assistant who helps users generate 3D human motion representations. The users will describe a motion, your job is to break it down into a short sequence of atomic physical actions. Show your reasoning inside <think> </think> and output motion in <Motion> </Motion> tags.

Response Format: Let me think step by step.

<think>...</think> <Motion>...</Motion>

A.2.3 MOTION-R1 W/O DECOMPOSED CoT

This form is used for training w/o decomposed CoT. No reasoning steps are involved, and the model directly maps textual descriptions to motion token sequences. This prompt is structurally simple and helps the model learn basic text-to-motion alignment without reasoning supervision.

You are an assistant who helps users generate 3D human motion representations. The users begin by describing the motion they envision. Show output motion in <Motion> </Motion> tags.
Response Format: <Motion>...</Motion>

A.3 EXPERIMENTAL SETTINGS

A.3.1 EVALUATION METRICS

Following Guo et al. (2022a); Zhang et al. (2023a); Wu et al. (2024), our evaluation metrics are summarized as follows:

1) *R-Precision*. It compares each motion sequence with 32 textual descriptions of one true match and 31 randomly sampled negative examples. Retrieval accuracy is measured by checking whether the correct description appears within the top-1, top-2, or top-3 nearest neighbors in the ranked list.

2) *FID*. FID measures the distributional similarity between real and generated motion features. Let (μ_r, Σ_r) and (μ_g, Σ_g) be the means and covariances of real and generated feature distributions, respectively. The FID score is computed as:

$$\text{FID} = \|\mu_r - \mu_g\|^2 + \text{Tr}(\Sigma_r + \Sigma_g - 2(\Sigma_r \Sigma_g)^{1/2}) \quad (6)$$

3) *Diversity*. To assess the variation within generated motion sequences, we follow the protocol introduced by Guo et al. Guo et al. (2022a). Specifically, we randomly sample S_{dis} pairs of motions from the generated set, and compute the average ℓ_2 distance between each pair’s motion features. Let $f_{\text{pred},i}$ and $f'_{\text{pred},i}$ denote the feature embeddings of the i -th sampled pair, the diversity is defined as:

$$\text{Diversity} = \frac{1}{S_{\text{dis}}} \sum_{i=1}^{S_{\text{dis}}} \|f_{\text{pred},i} - f'_{\text{pred},i}\|_2 \quad (7)$$

In our implementation, we set $S_{\text{dis}} = 300$ to ensure stable and comparable estimates across methods.

4) *Multimodal Distance (MM-Dist)*. MM-Dist evaluates the alignment between generated motions and their corresponding text descriptions. It is defined as the cosine similarity between the embeddings of a generated motion and its conditioning text, extracted using a pretrained joint encoder.

5) *Multimodality (MModality)*. Multimodality assesses the model’s ability to generate diverse motions conditioned on the same textual input. It is computed by generating multiple motions from a single description and measuring the average pairwise Euclidean distance between their feature embeddings. Higher scores indicate a greater ability to model one-to-many mappings between text and motion.

A.3.2 TRAINING DETAILS

We first fine-tune the pre-trained model on MotionCoT data using supervised learning with a batch size of 8 and a learning rate of 1×10^{-4} , scheduled by cosine decay.

Building on this, GRPO training is implemented with group size $G = 8$, clipping range $\varepsilon = 0.2$, and KL penalty coefficient $\beta = 0.001$ for stable policy optimization.

A.3.3 EXPERIMENTS COMPUTE RESOURCES

All experiments were conducted on a server with 8xNVIDIA H20 GPUs. The SFT training took approximately 2 hours on 8 GPUs, while GRPO-based reinforcement learning required around 4 hours under the same configuration. Evaluation on HumanML3D and KIT-ML datasets consumed about 1 GPU-hours per run, repeated across 20 trials for statistical robustness.

Inference time analysis was conducted under the same NVIDIA H20 and prompt conditions. Over 10 runs, our method takes 2.23 seconds while MotionLLM Wu et al. (2024) takes 2.11 seconds, showing no significant difference in inference time. Despite comparable inference speed, our method achieves superior performance in both quantitative and qualitative evaluations.

A.4 QUALITATIVE RESULTS ON BABEL

Results on **BABEL**. Table 3 reports results on the BABEL Punnakkal et al. (2021) dataset, which contains long, multi-label activity annotations. Motion-R1 outperforms prior methods across all metrics. It achieves the highest R-Precision (**0.536** \pm .004), surpassing InfiniDreamer (0.522 \pm .008)

and other baselines, indicating stronger text–motion semantic alignment. In terms of motion fidelity, Motion-R1 attains a substantially lower FID of $0.53 \pm .006$, nearly halving the best baseline ($1.14 \pm .05$ from DoubleTake/InfiniDreamer). For motion–language embedding distance, Motion-R1 also sets the best score ($6.16 \pm .141$), suggesting better cross-modal consistency. Moreover, its Diversity ($8.90 \pm .095$) exceeds even ground-truth motion (8.52), reflecting the ability to synthesize varied yet realistic motions.

Overall, these results demonstrate that Motion-R1 generalizes effectively to BABEL, producing semantically accurate, diverse, and high-fidelity motions under complex multi-label activity settings.

Table 3: **Quantitative results of Motion-R1 on BABEL Punnakkal et al. (2021)**. The evaluations are conducted 20 times to obtain a 95% confidence interval. Best results are highlighted in **bold** and the second best in underline.

Methods	R-Precision \uparrow	FID \downarrow	MM-Dist \downarrow	Diversity \uparrow
Ground Truth	$0.629 \pm .001$	$0.0004 \pm .00$	$3.51 \pm .01$	$8.52 \pm .09$
TEACH Athanasiou et al. (2022)	$0.461 \pm .012$	$1.43 \pm .04$	$7.93 \pm .01$	$7.71 \pm .11$
DoubleTake Shafir et al. (2023)	$0.483 \pm .009$	<u>$1.14 \pm .05$</u>	$6.97 \pm .01$	<u>$8.28 \pm .09$</u>
DiffCollage Zhang et al. (2023b)	$0.487 \pm .009$	$1.83 \pm .05$	$6.74 \pm .01$	$7.89 \pm .11$
InfiniDreamer Zhuo et al. (2024)	<u>$0.522 \pm .008$</u>	<u>$1.14 \pm .11$</u>	<u>$6.35 \pm .01$</u>	$7.97 \pm .05$
Motion-R1	$0.536 \pm .004$	$0.53 \pm .006$	$6.16 \pm .141$	$8.90 \pm .095$

A.5 USER STUDY

To evaluate the perceptual quality of our generated motions, we conduct a user study comparing our method with baseline approaches. We randomly select 100 composite action descriptions as test samples, where each description’s generated results from three methods (MotionAgent Wu et al. (2024), MoMask Guo et al. (2024), ours) are displayed side-by-side. Fifty users independently select the best method for semantic consistency and motion fluency respectively for each description. The results are shown in Table 4, demonstrating that our method significantly outperforms baselines in both semantic consistency and motion fluency.

Table 4: **User study on semantic consistency and motion fluency**. 100 composite action descriptions were evaluated by 50 users, who independently selected the best method for each dimension. Best results are highlighted in **bold** and the second best in underline.

Methods	Semantic Consistency	Motion Fluency
MotionAgent Wu et al. (2024)	<u>28.4%</u>	<u>32.6%</u>
MoMask Guo et al. (2024)	25.8%	28.2%
Motion-R1	45.8%	39.2%

A.6 LIMITATIONS

Despite its advantages, Motion-R1 has limitations. The Decomposed CoT Data Engine relies on general-purpose LLMs, which may produce noisy or suboptimal plans under ambiguous instructions. Furthermore, while RL Binding streamlines policy optimization, careful design of motion- and semantic-level rewards remains crucial. Future work will explore adaptive reward learning and interactive feedback mechanisms to further enhance motion quality and robustness.